

See discussions, stats, and author profiles for this publication at: <https://www.researchgate.net/publication/27264516>

Formation of unusual 10-petal BaSO₄ structures in the presence of a polymeric additive

ARTICLE

Source: OAI

CITATIONS

3

READS

39

4 AUTHORS, INCLUDING:



Helmut Cölfen

Max Planck Institute for Chemistry

294 PUBLICATIONS **13,310** CITATIONS

SEE PROFILE



Yitzhak Mastai

Bar Ilan University

120 PUBLICATIONS **2,316** CITATIONS

SEE PROFILE

Formation of Unusual 10-Petal BaSO₄ Structures in the Presence of a Polymeric Additive

Helmut Cölfen,* Limin Qi,[#] Yitzhak Mastai, and Lars Börger[‡]

Max-Planck-Institute of Colloids and Interfaces, Colloid Chemistry, Research Campus Golm, D-14424 Potsdam, Germany

Received February 12, 2002; Revised Manuscript Received March 6, 2002

ABSTRACT: In this work, the formation of unusual flowerlike structures with 10-petals composed of BaSO₄ single crystalline platelets is described. The structures are obtained at pH 5 in an aqueous solution in the presence of a double hydrophilic block copolymer poly(ethylene oxide)-*block*-sulfonated poly(ethylene imine) (PEO-*b*-PEI-SO₃H) by site-specific polymer adsorption. The exposed faces are identified, the atomar surface structures of these faces are calculated, and preferred faces for polymer adsorption are found. A model for the growth of the unusual 10-petal BaSO₄ structures is presented which is based on the nucleation of primary particles, secondary growth of the petals, and finally layer wise petal overgrowth.

Introduction

The synthesis of inorganic materials having a specific size, modification, and morphology is a key aspect in fields as diverse as modern materials, catalysis, medicine, electronics, ceramics, pigments, and cosmetics.^{1–4} Compared with the size control, the morphology control or morphogenesis is more demanding to achieve by means of classical procedures of colloid chemistry,⁵ although it has already been tried for a long time to influence crystal morphologies by empirically adding additives, but the knowledge about these processes is still limited. Therefore, especially complex crystalline forms deviating from the normal structure dictated by the unit cell are still most difficult to realize in a controlled manner. In that respect, mimicking of biomineralization processes offers a significant potential for crystal design due to the highly controlled crystal growth and morphogenesis as well as hierarchical structuration of crystalline building units, often over several length scales, in biomineralization.⁶

Recently, a new class of functional polymers, the so-called double-hydrophilic block copolymers (DHBCs),^{7–9} was developed for mineralization purposes. These polymers consist of one hydrophilic block designed to interact strongly with the appropriate inorganic minerals and surfaces, and another hydrophilic block that does not interact or only weakly interacts with mineral surfaces and mainly promotes solubilization in water. Owing to the separation of the binding and the solvating moieties, these polymers turned out to be extraordinarily effective in crystallization control including calcium carbonate,^{8–12} calcium phosphate,¹³ barium sulfate,^{14–16} barium chromate,¹⁷ zinc oxide,¹⁸ ice,¹⁹ and also organic crystals such as calcium- and ammonium tartrate where

even a partial racemate separation induced by crystallization could be achieved.²⁰ They also turned out to be effective additives for the formation of nanoparticles of various noble metals such as Au, Pt, and Pd which were obtained by reduction of their complex salts in the formed block copolymer micelles^{21–23} as well as Ag nanowires.²⁴ In case of the semiconductor CdS, even a size control and stabilization against photooxidation by a simple precipitation reaction in water could be achieved.²⁵

However, despite the considerable amount of experimental data which document the extraordinary influence of DHBCs on the crystallization of organic and inorganic crystals and the formation of unusual well-defined superstructures from nanoparticles, still very little is known about the formation of either the superstructures or observed unusual crystal morphologies. Only three recent reports are known up to now, which try to establish a mechanism for the superstructure formation from CaCO₃ nanoparticles^{12,26} or for BaSO₄ single crystal fiber formation.¹⁶ This is mainly a consequence of the difficulties, to analyze these processes. In this paper, we want to report on the formation mechanism of unusual 10-petal BaSO₄ structures which have already been observed in our earlier work¹⁴ to shed more light on the crystal design processes by DHBCs. The found 10-petal symmetry is remarkable in a way that the only rotational symmetries that are possible for a crystal are 2-, 3-, 4-, and 6-fold rotations being among the most well-known consequences of periodicity. Five-fold rotations (and any *n*-fold rotation for *n* > 6) are incompatible with periodicity. Five-fold symmetry was considered to be impossible in real materials until it was discovered by Shechtman in the early 1980s.²⁷ The discovery led to the exploration of an entirely new area, the Quasicrystals.^{28,29} Quasicrystals are materials that do not have a periodic lattice structure but still display subtle long-range order, such as “five-fold” symmetry, that is not possible in regular crystals and they are usually found in metallic alloys such as Al-TM (TM = Ir, Pd, Pt, Os, Ru, Rh, Mn, Fe, Co, Ni, Cr).

* Corresponding author: Dr. habil. Helmut Cölfen, Max-Planck Institute of Colloids and Interfaces, Colloid Chemistry, Research Campus Golm, D-14424 Potsdam, Tel.: ++49-331-5679513; fax: ++49-331-5679502; e-mail: Coelfen@mpikg-golm.mpg.de, <http://www.mpihg-golm.mpg.de/kc/coelfen/> & <http://www.mpihg-golm.mpg.de/kc/people/Coelfen/en/index.html>.

[#] Prof. Qi's present address is College of Chemistry, Peking University, Beijing 100871 (P.R. China).

[‡] Dr. Börger's present address is BASF AG, Polymer Research, G201, D-67056 Ludwigshafen, Germany.

Experimental Section

Sulfonated poly(ethylene oxide)-*block*-poly(ethylene imine) (PEO-*b*-PEI-SO₃H) and poly(ethylene oxide)-*block*-poly(ethylenediamine tetra acetic acid) were synthesized as described elsewhere.^{8,9} The PEO-*b*-PEDTA precursor polymer has also been modified by addition of one fluorescein label per polymer chain. To label the precursor polymer 50 mg of (PEO-*b*-PEDTA) ($M_{w, \text{theoretical}} = 7000$ g/mol) were linked together in analogy to the procedure described elsewhere.³⁰ The polymer was dissolved in 6 mL of H₂O (pH = 8.1), and then a solution of 4 mg of fluorescein isothiocyanate (FITC, Aldrich) in 500 μ L of dimethyl sulfoxide (DMSO) was added. The reaction solution was stirred for 12 h in darkness at room temperature. The surplus FITC was removed by exhaustive dialysis against a water/DMSO mixture (12:1).

The "synthesis" of the BaSO₄ particles involved simultaneous addition of 0.5 M Ba(Ac)₂ (Aldrich, A. R. grade) and 0.5 M (NH₄)₂SO₄ (Aldrich, A. R. grade) to 300 mL of 1 g/L aqueous PEO-*b*-PEI-SO₃H solution, which was adjusted to a desired pH using 1 M NaOH or HCl before injection of reactants, in a double jet reactor⁸ tempered at 25 °C. The continuous reactant supply of 0.5 mL/h leading to a BaSO₄ formation rate of 1.39×10^{-5} M/min was stopped when the solution became obviously turbid. The precipitates were left to stand in their mother solutions for at least 24 h to ensure equilibration.

Scanning electron microscopy (SEM) was performed with a DSM 940 A (Carl Zeiss, Jena) microscope. Conventional TEM bright and dark-field imaging and electron diffraction were carried out with a Phillips CM-120 microscope, operating at 120 kV. Electron diffraction patterns were taken with or without a selected area aperture; in the cases in which an aperture was used, the aperture diameter was 0.9 mm and the patterns were obtained at a camera length of 900 mm. High-resolution TEM (HRTEM) images were taken at a magnification of 500000 \times or more using an objective lens of 0.9 mm. In TEM dark field imaging mode, we used a single diffracted beam to form the image. All areas on the surface that contribute to the existence of this spot, namely, crystals with the same crystal structure and orientation, appear bright in the image, all other areas appear dark.

The crystal morphology calculations were made with the SHAPE professional Vers. 5.01 Software by Eric Dowty and the calculations of the atomar crystal surface structures by appropriate cleavage of the crystal lattice with the *Cerius2* software by Accelrys.

Results and Discussion

The default morphology of BaSO₄ under the chosen conditions without an additive is rectangular tablets over a wide range of pH.^{14,15} If BaSO₄ is crystallized in the presence of 1 g/L PEO-*b*-PEI-SO₃H at pH 5 in a double jet experiment where the solution supersaturation is continuously increased, a complicated flowerlike morphology is obtained, whereas at pH 9, the morphology is more irregular (Figure 1).¹⁴ The irregular morphology at pH 9 may be explained by the fact that at alkaline pH, the barite surfaces with an isoelectric point of 3.9³¹ are negatively charged resulting in a repulsion of the negatively charged polyelectrolyte block, consequently, drastically minimizing the polymer control of the crystal growth. Therefore, these conditions were not further investigated, and it was focused on the flower morphologies at the acidic pH 5.

The flower morphologies exhibit 10 petals which themselves show layers of overgrown material suggesting a multistep growth mechanism. However, the observed symmetry of 10 cannot be explained with a primary crystal exhibiting the usual barite morphology. To shed more light onto the formation mechanism, thin

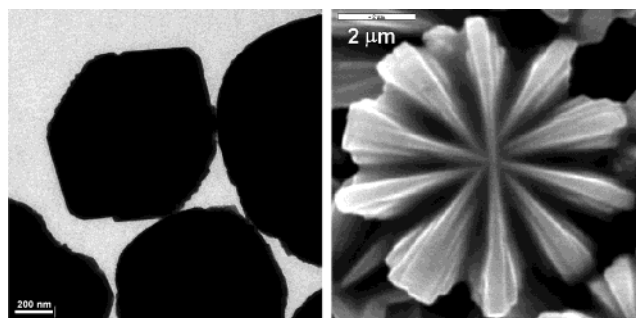


Figure 1. TEM and SEM micrographs of BaSO₄ precipitated in the presence of 1 g/L PEO-*b*-PEI-SO₃H at pH 9 (left) and pH 5 (right).

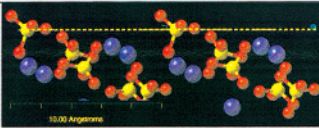
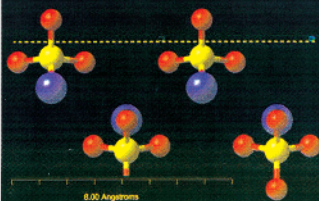
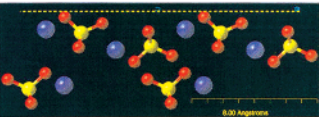
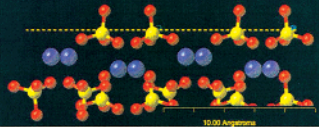
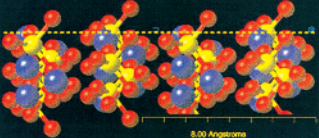
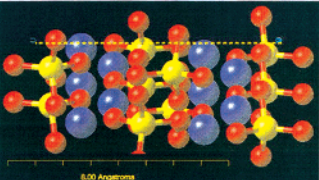
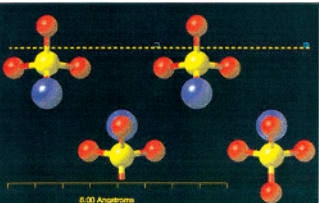
cuts of the epoxy embedded flower structures were made but the flowers turned out to be very fragile structures so that no thin cut could be obtained without breaking the structures. Nevertheless, electron diffraction (ED) on these thin cuts revealed that all petals start from a center point and that the flowers are orthorhombic BaSO₄ (a , b , c = 8.909, 5.467, and 7.188 Å Figure 2).

Despite the fractured flower structure, ED showed spots on diffraction rings suggesting a single crystalline structure of the flowers. The diffraction rings were indexed and showed that the flower structures exhibit higher index faces (Table 1). It should be noted that the intensity of the diffraction ring (400) in our samples is rather high compared to the bulk sample (which is about 4% as reported in the powder X-ray diffraction card 24-1035). This indicates a possible orientation of the petals or an exposed 200/400 face.

To identify possible polymer adsorption faces, the atomar surface structure was calculated by cleaving the crystal lattice parallel to the selected face. The results are given in Table 1 and show that the 400 face as well as the equal 200 face should be favored for adsorption of the sulfonate functionalized block copolymer polyelectrolyte block. On these faces, the sulfate ions are exposed in a favorable geometrical condition for either their lattice replacement by the structurally closely related sulfonate groups or the completion of unsaturated Ba²⁺ coordination sites. If polymer adsorption preferably takes place onto these faces, they can be expected to be large in the resulting crystal morphology due to their hindered growth. Indeed, the intensity of the 400 diffraction was much higher than should be expected, indicating an expressed face in the morphology (Figure 2 right). With the planes in Table 1, a possible crystal morphology could be calculated by applying the constraint of a large 400 surface area. The results are shown in Figure 3.

It can be seen that with the enhanced 400 surface, a morphology of a primary crystal is obtained which exhibits 10 faces parallel to the crystal a -axis. All these faces show a more unfavorable condition for tridentate sulfate ion replacement or saturation of the Ba²⁺ lattice ion coordination sites compared to 200/400 and thus should be less favorable for polymer adsorption. Assuming a secondary nucleation of the petals on the faces parallel to the a -axis in Figure 3, the 10-petal flower like structure in Figure 1 can be obtained if the 111 and 140 faces are neglected as they are too small to become significant for secondary nucleation. This symmetry is

Table 1. Indexing of the Diffraction Rings from ED (from Center to Outside) on Thin Cuts of the Flowerlike Structure and the Calculated Atomar Surface Structures of These Faces^a

Ring	d-spacing (Å)	Plane	Atomar surface structure
1	3.852	111	
2	3.510	200	
3	2.772	002	
4	2.340	022	
5	2.170	140	
6	2.106	041	
7	1.769	400	

^a The crystal surface faces the top of the page and is indicated by a yellow dashed line. The blue spheres represent Ba²⁺.

remarkable because a direct 10-fold crystal symmetry is forbidden and only rarely found in quasicrystal alloys.^{27–29,32,33}

A closer examination of the petals by HRTEM reveals that each petal is a single BaSO₄ crystal evident from the parallel lattice fringes throughout the petal (Figure 4, left). The lattice spacing of 3.42 Å is consistent with the 200 face so that the petals appear to be elongated along the barite 001 *c*-axis (Figure 4 left).

This is confirmed by selected area electron diffraction (SAED) on the end of a petal in an orientation as in Figure 4 (right) which was thin enough to show a dot diffraction pattern (data not shown) where two strong dot patterns correspond to the 002 and 200 planes

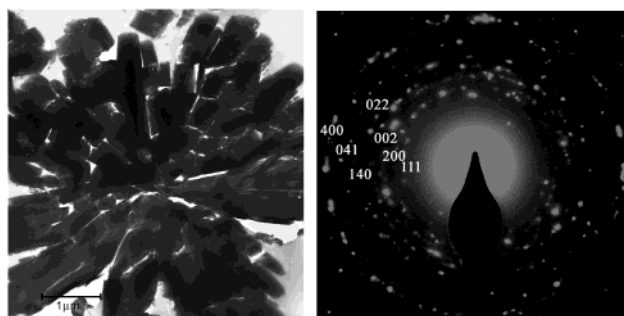


Figure 2. TEM (left) and ED (right) on thin cuts of the flowerlike structures.

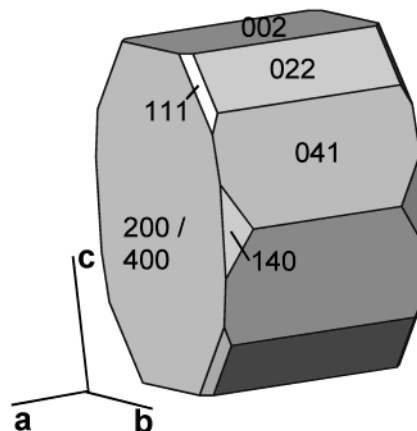


Figure 3. Calculated morphology of a possible primary barite crystal according to the results from ED (Table 1).

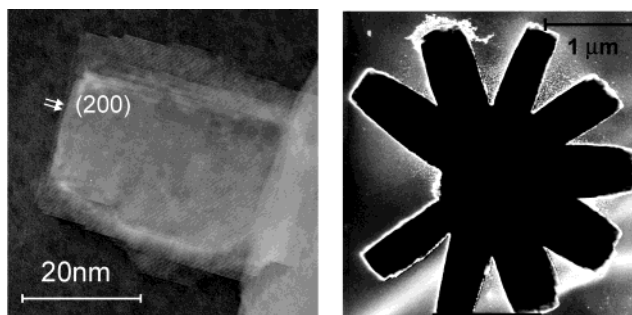


Figure 4. EM analysis of the BaSO₄ flowerlike structures. Left: HRTEM of a petal, Right: dark field TEM of an entire particle with the defect of one missing petal constructed from the diffraction dot of the 200 plane.

supportive of a barite crystal elongated along the 001 *c*-axis. It could be revealed by dark field TEM that each petal adopts this orientation (Figure 4 right, illumination of all petals). The third face of the petals should then be 020 due to symmetry reasons as the petals exhibit only three main faces that are perpendicular to each other. According to the atomar surface structure of the 020 face, polymer adsorption is not favored (data not shown).

Figure 4 right shows that the secondary growth of the petals on the primary crystal does not adopt the orientation of the underlying crystal faces by epitaxy. Otherwise, all petals should exhibit different faces from the exclusively detected 200 and 002. Further support for this comes from the finding that the angles between the petals appear to be almost equal in the SEM picture

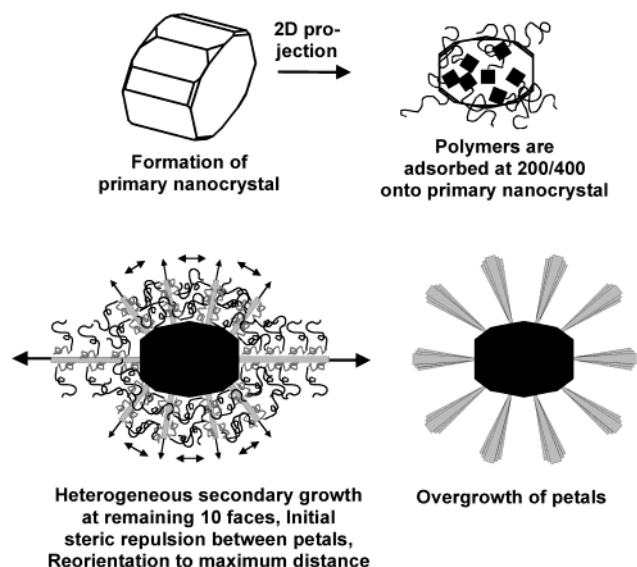


Figure 5. Proposed growth mechanism for the flowerlike BaSO_4 morphology shown in Figure 1. For clarity reasons, the figure is not drawn to scale, and the primary nanocrystal is drawn in an overproportional size.

in Figure 1, whereas the morphology of the proposed primary crystal in Figure 3 suggests them to be different. A more detailed analysis of nine SEM pictures concerning their match with the 2D morphology projection of the 10-petal structure resulting from the primary crystal in Figure 3 or a constant angle symmetry confirmed the constant angle between the petals of about 36° . These findings suggest that the underlying growth mechanism of the flowers must be more complicated than the nucleation of a primary crystal which then defines the angles between the crystals growing in a second step by epitaxy. The growth model proposed for the flower growth of BaSO_4 is shown in Figure 5.

This model is based upon the following experimental observations:

ED data (Figure 2) give six different crystal faces displayed in Table 1 consistent with a primary crystal displayed in Figure 3.

The existence of a primary crystal is suggested by the fact that all of the 10 petals originate in a single point (Figure 1, right) as otherwise, this would suggest a forbidden 10-fold symmetry for the observed single crystals (Figure 2, right).

The primary crystal must be of a size in the nanometer regime as it was never observed in TEM thin cuts displaying the micrometer regime (Figure 2, left).

The 10 petals have equal angles between each other, meaning that they cannot grow epitactically onto the primary crystal proposed in Figure 3, thus suggesting a heterogeneous secondary growth of the petals onto a primary crystal.

All petals exhibit equal crystallographic orientations (Figure 4, right) and appear to be elongated along the barite c -axis. This is also supportive of a secondary growth process.

One pair of petals is interconnected (see Figure 1, right), and the other eight are not, which suggests a slightly preferred growth of these two petals.

200/400 are exposed faces (Figure 2, right), which is caused by their atomar surface structure favoring a

replacement of sulfate ions by the structurally related polymer functional sulfonate groups or the completion of surface Ba^{2+} coordination sites.

An overgrowth of the petals is observed (Figure 1, right), which suggests a tertiary growth process.

Taking all the above experimental observations into account, we suggest that nanometer-sized primary crystals of the shape displayed in Figure 3 are nucleated at the high supersaturation following the induction period of barite crystallization in the presence of DHBCs.¹⁶ Despite the continuous slow reactant addition, the homogeneous nucleation of the primary crystals lowers the supersaturation considerably after the point of homogeneous primary crystal nucleation. During the primary crystal growth, the 200/400 faces are exposed according to polymer adsorption due to sulfate ion replacement or the completion of the Ba^{2+} surface ion coordination sites, but the development of the other crystal faces shown in Figure 3 also has to be considered. It has to be noted that from the six different faces of the suggested primary crystal in Table 1, four are directly structurally related or are out of the eight which are thought to be important for the growth of barite, namely, 001; 010; 011; 101; 111; 200; 210; 211.³⁴ Just one of them (002) is among the morphology determining surfaces 001; 210; 101; 211; and 020.³⁵ The higher index faces 400, 041, and 140 are uncommon. Whereas 400 is structurally equal to 200, the 140 face does not play a predominant role due to its minor expression as indicated in Figure 3. In that respect, it is interesting to note that very recently a conformationally flexible macrocycle was designed, which interacts with every barite face, adsorbs, and thus inhibits their growth.³⁶ This macrocycle was designed according to computer simulations for the optimum binding to all important barite growth faces. This leads to a loss of all barite faces so that spherical single crystals are obtained. This is the opposite effect of the generation or expression of crystal faces through polymer interaction which was observed here.

Once the primary crystals are nucleated, the barite solubility product is not exceeded anymore so that further homogeneous nucleation cannot occur anymore despite the slow barite reactant addition and the formation of barite nanoparticles at the connection point of the jets which will dissolve until a sufficient supersaturation is reached again. Thus, heterogeneous nucleation comes into play as it generally requires a lower activation energy compared to homogeneous nucleation. With respect to the proposed primary nanocrystal structure in Figure 3, this means a secondary growth on the faces parallel to the barite a -axis by heterogeneous nucleation. As the 002 face is commonly found as the end face for all petals, the better atomar match for the nucleation of the petals on these faces compared to the other eight parallel to the crystal a -axis of the primary crystal, serving as heterogeneous nucleation sites (Figure 3), suggests the preferred heterogeneous petal growth onto the 002 faces of the primary crystal. Here, the activation energy for heterogeneous nucleation of a petal is assumed to be lower compared to the other faces due to partial epitaxial match. However, we have to state that this process breaks the symmetry of the primary crystal.

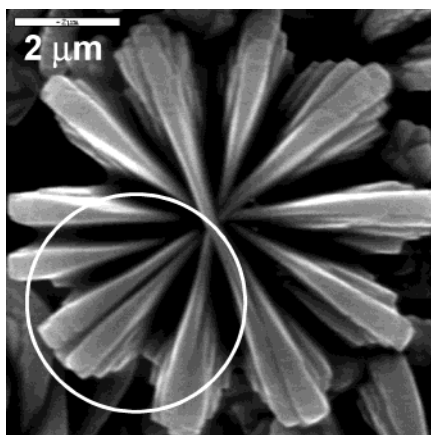


Figure 6. Defects in the BaSO₄ flower structure. Growth of two petals at a growth site for a single petal.

Once the petals have started to grow heterogeneously onto the 002 faces of the primary crystal, the other eight petals start to grow simultaneously by heterogeneous nucleation with an equal growth probability. The continuous supply of BaSO₄ for further growth is maintained by the continuous reactant addition during the double jet process. Here, it is important to note that heterogeneous nucleation happens on all faces parallel to the barite *a*-axis, leaving the 200/400 faces with adsorbed polymer unaffected and thus exposed. This means in result that a symmetry break occurs during heterogeneous nucleation onto the primary crystal according to Figure 5. The petals were found to exhibit equal angles of about 36° between each other, which is in contrast to an epitactical growth onto the suggested primary crystal (Figure 3) so that a directing force has to be discussed for this. This may be the steric repulsion between the early developing petals generated by the PEG block pendant to the adsorbed functional block on the 200/400 faces of the developing petals. As this steric repulsion layer is only in the range of 3–5 nm, it is clear that it can only affect the very early secondary growth stages. Furthermore, a charge contribution originating from polyelectrolyte adsorption completing the Ba²⁺ coordination sites may be discussed.

When the petals are developed and the entire crystal structure has grown, a tertiary growth process sets in evident as a petal overgrowth. This overgrowth can be repeated several times (Figure 1 right, Figure 6). This is likely to be the result of the slowly continued reactant addition and implies that the adsorbed polymer on 200/400 does not hinder crystal overgrowth. If the polymer would be statically adsorbed, it would be included into the crystal which should lead to defect structures that are not generally observed on the petals. More likely appears the second possibility, that the polymer adsorption is a dynamic adsorption/desorption process where the polymer is present on the crystal surface on a time average³⁷ and thus allows for an epitactical crystal overgrowth.

The flowers can show defects when two petals grow at a position, where normally only one petal would grow (Figure 6). This is a clear indication for the heterogeneous secondary petal growth.

The nucleation of two petals instead of one can take place if two petals are simultaneously nucleated on a

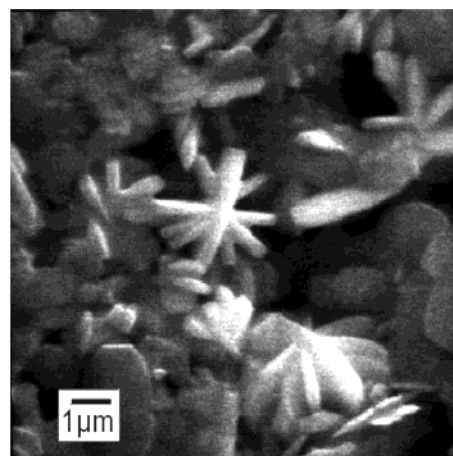


Figure 7. SEM micrographs of BaSO₄ precipitated in the presence of 1 g/L PEO-*b*-PEDTA with a fluorescein label at pH 5.³⁸

single face of the primary crystal. Due to the confined space on the nucleation face on the primary crystal, these petals grow together so that they cannot alter their orientation to minimize the repulsion between the petals. It is remarkable that this effect is not observed with the two opposite interconnected petals, which is an indication for their preferred growth compared to the other petals.

Defect flower structures were also observed for BaSO₄ precipitation experiments in the presence of PEO-*b*-PEDTA with one fluorescein label per polymer chain. However, here, the effect is opposite to the above-discussed one in the respect that petals are missing instead of the nucleation of two petals instead of one. Also, some platelets are observed beside the incomplete flower structures (Figure 7).

The hydrophobic fluorescein label decreases the interaction of the EDTA block with the crystal surface so defect flowerlike morphologies were now obtained (Figure 7) instead of the expected dumbbell morphologies for PEO-*b*-PEDTA.¹⁴ Apparently, the polymer–crystal interaction is not high enough anymore to stabilize amorphous nanoparticles which are discussed as precursor particles for the higher order assembly to dumbbell morphologies.¹² Instead, macroscopic crystals are obtained in agreement with the mechanism suggested by Cölfen and Qi,²⁶ but the lot of defect structures (Figure 7) indicates a little selectivity of the hydrophobically modified PEO-*b*-PEDTA with carboxy functional groups which is not unexpected. It is remarkable that defect flowerlike BaSO₄ structures, which differ from those observed in this study in the respect that they do not have 10 petals, are also obtained in the presence of PEO homopolymer or when the polymer–crystal interaction of a the PMAA block of PEO-*b*-PMAA was stopped by full PMAA protonation at pH 3.¹⁵ This is also supportive of the view that defect flower like structures can be observed, when the polymer interaction is weak and not very selective with respect to the barite crystal faces.

Conclusions

It could be shown that site-selective polymer adsorption can lead to very unusual crystal structures com-

posed of single crystals. Crystalline BaSO₄ structures exhibiting 10 equally ($\approx 36^\circ$) spaced petals as a result of a selective adsorption of PEG-*b*-PMAA-SO₃H onto barite 200/400 faces suggest a multistep growth process on a nanometer-sized primary crystal. Computer calculations of the atomar surface structures of the crystal faces, identified by electron diffraction of a thin cut of the crystal, reveal that the 200/400 faces expose their sulfate ions in a favorable orientation for their replacement by the structurally similar sulfonate groups of the polymer or the completion of Ba²⁺ coordination sites by the polymer sulfonate groups. Thus, polymer adsorption is favored at these faces so that they become exposed in the petal morphology. Heterogeneous nucleation onto the nanometer-sized primary crystal, constrained in the very early stages by the stabilizing PEO chains then leads to an equalization of the angle between the secondarily growing petals due to steric repulsion between the PEO stabilizing chains with a range of 3–5 nm. The final result is a micron-sized single crystalline flower structure with 10 equally spaced petals due to overgrowth of a crystal structure, already predefined in the primary nanocrystal, to the finally observed unusual 10-petal crystalline BaSO₄ structure. Heterogeneous nucleation of the single crystalline petals is already clearly favorable from the thermodynamic viewpoint after the initial high supersaturation by polymeric crystallization inhibition is lowered by the homogeneous nucleation of the primary nanoparticles. A strong support for the heterogeneous petal nucleation are the observed crystal defect structures where two petals are nucleated instead of one. Finally, the petals are overgrown in a third process, which implies a dynamic polymer adsorption/desorption equilibrium onto the 200/400 faces.

Summarizing, it can be stated that a complex multistep growth process can lead to crystalline BaSO₄ particles showing an unusual 10-fold symmetry, which is forbidden for a single crystal. This outlines the possibilities of crystal engineering by site-selective polymeric additives to generate very complex crystal morphologies as a (still rather imperfect) mimic of some biomineralization processes.

Acknowledgment. We thank the Max-Planck Society and DFG(SFB 448) for financial support of this work. Y.M. thanks the Minerva foundation for a Minerva scholarship. H.C. acknowledges financial support by the Dr. Herrman-Schnell foundation. We also thank Rona Pitschke for her skillful preparation of the crystal thin cuts.

References

- (1) Mann, S.; Ozin, G. A. *Nature* **1996**, *382*, 313.
- (2) Yang, H.; Coombs, N.; Ozin, G. A. *Nature* **1997**, *386*, 692.
- (3) Ahmadi, T. S.; Wang, Z. L.; Green, T. C.; Henglein, A.; El-Sayed, M. A. *Science* **1996**, *272*, 1924.
- (4) Matijevic, E. *Curr. Opin. Colloid Interface Sci.*, **1996**, *1*, 176.
- (5) Matijevic, E. *Chem. Mater.* **1993**, *5*, 412.
- (6) Mann, S.; Webb, J.; Williams R. J. P., Eds.; *Biomineralisation, Chemical and Biochemical Perspectives*; VCH: Weinheim, 1989.
- (7) Cölfen, H. *Macromol. Rapid Commun.* **2001**, *22*, 219.
- (8) Sedlak, M.; Antonietti, M.; Cölfen, H. *Macromol. Chem. Phys.* **1998**, *199*, 247.
- (9) Sedlak, M.; Cölfen, H. *Macromol. Chem. Phys.* **2001**, *202*, 587.
- (10) Cölfen, H.; Antonietti, M. *Langmuir* **1998**, *14*, 582.
- (11) Marentette, J. M.; Norwig, J.; Stockelmann, E.; Meyer, W. H.; Wegner, G. *Adv. Mater.* **1997**, *9*, 647.
- (12) Cölfen, H.; Qi, L. *Chem. Eur. J.* **2001**, *7*, 106.
- (13) Antonietti, M.; Breulmann, M.; Göltner, C. G.; Cölfen, H.; Wong, K. K.; Walsh, D.; Mann, S. *Chem. Eur. J.* **1998**, *4*, 2493.
- (14) Qi, L.; Cölfen, H.; Antonietti, M. *Angew. Chem., Inter. Ed.* **2000**, *39*, 604.
- (15) Qi, L.; Cölfen, H.; Antonietti, M. *Chem. Mater.* **2000**, *12*, 2392.
- (16) Qi, L.; Cölfen, H.; Antonietti, M.; Li, M.; Hopwood, J. D.; Ashley, A. J.; Mann, S. *Chem. Eur. J.* **2001**, *7*, 3526.
- (17) Yu, S. H.; Cölfen, H.; Antonietti, M. **2002**, *Chem. Eur. J.*, accepted for publication.
- (18) Öner, M.; Norwig, J.; Meyer, W. H.; Wegner, G. *Chem. Mater.* **1998**, *10*, 460.
- (19) Mastai, Y.; Rudloff, J.; Cölfen, H.; Antonietti, M. *Chem. Phys. Chem.* **2002**, *1*, 119.
- (20) Mastai, Y.; Sedlak, M.; Cölfen, H.; Antonietti, M. *Chem. Eur. J.* **2002**, accepted.
- (21) Bronstein, L. M.; Sidorov, S. N.; Gourkova, A. Y.; Valetsky, P. M.; Hartmann, J.; Breulmann, M.; Cölfen, H.; Antonietti, M. *Inorg. Chim. Acta* **1998**, *280*, 348.
- (22) Sidorov, S. N.; Bronstein, L. M.; Valetsky, P. M.; Hartmann, J.; Cölfen, H.; Schnablegger, H.; Antonietti, M. *J. Colloid Interface Sci.* **1999**, *212*, 197.
- (23) Bronstein, L. M.; Sidorov, S. N.; Valetsky, P. M.; Hartmann, J.; Cölfen, H.; Antonietti, M. *Langmuir* **1999**, *15*, 6256.
- (24) Zhang, D. B.; Qi, L.; Ma, J. M.; Cheng, H. M. *Chem. Mater.* **2001**, *13*, 2753.
- (25) Qi, L.; Cölfen, H.; Antonietti, M. *Nano Lett.* **2001**, *1*, 61.
- (26) Cölfen, H.; Qi, L. *Prog. Colloid Polym. Sci.* **2001**, *117*, 200.
- (27) Shechtman, D.; Blech, I.; Gratias, D.; Cahn, J. W. *Phys. Rev. Lett.* **1984**, *53*, 1951.
- (28) Shechtman, D.; Lang, C. *MRS Bulletin* **1997**, Vol. 22, No. 11, 40.
- (29) Janot, C. *Quasicrystals: A Primer*, 1994, 2nd ed., Clarendon Press: Oxford.
- (30) von Klitzing, R.; Möhwald, H. *Langmuir* **1995**, *11*, 3554.
- (31) Yousef, A. A.; Bibawy, T. A.; Malati, M. A. *Chem. Ind.-London* **1977**, *6*, 229.
- (32) Hofmeister, H. *Cryst. Res. Technol.* **1998**, *33*, 3.
- (33) Gryaznov, V. G.; Heydenreich, J.; Kaprelov, A. M.; Nepijko, S. A.; Romanov, A. E.; Urban, J. *Cryst. Res. Technol.* **1999**, *34*, 1091.
- (34) Hartmann, P.; Perdock, W. G. *Acta Crystallogr.* **1955**, *8*, 524.
- (35) Hopwood, J. D. Ph.D. Thesis, University of Bath, 1996.
- (36) Coveney, P. V.; Davey, R.; Griffin, J. L. W.; He, Y.; Hamlin, J. D.; Stackhouse, S.; Whiting, A. *J. Am. Chem. Soc.* **2000**, *122*, 11557.
- (37) Peytcheva, A.; Antonietti, M. *Angew. Chem., Intl. Ed.* **2001**, *40*, 3380.
- (38) Börger, L. Ph.D. Thesis, Potsdam, 2000.

CG025507V